Lab on a Chip

Dynamic Article Links

Cite this: *Lab Chip*, 2012, **12**, 4168–4177

www.rsc.org/loc

PAPER

Continuous flow multi-stage microfluidic reactors *via* hydrodynamic microparticle railing†

Ryan D. Sochol,*[ac] Song Li,[b] Luke P. Lee[bc] and Liwei Lin[ac]

Received 28th May 2012, Accepted 18th July 2012
DOI: 10.1039/c2lc40610a

''Multi-stage'' fluidic reactions are integral to diverse biochemical assays; however, such processes typically require laborious and time-intensive fluidic mixing procedures in which distinct reagents and/or washes must be loaded sequentially and separately (*i.e.*, one-at-a-time). Microfluidic processors that enable multi-stage fluidic reactions with suspended microparticles (*e.g.*, microbeads and cells) to be performed autonomously could greatly extend the efficacy of lab-on-a-chip technologies. Here we present a single-layer microfluidic reactor that utilizes a microfluidic railing methodology to passively transport suspended microbeads and cells into distinct, adjacent laminar flow streams for rapid fluidic mixing and assaying. Four distinct molecular synthesis processes (*i.e.*, consisting of 48 discrete fluidic mixing stages in total) were accomplished on polystyrene microbead substrates (15 μm in diameter) in parallel, without the need for external observation or regulation during device operation. Experimental results also revealed successful railing of suspended bovine aortic endothelial cells (approximately 13 to 17 μm in diameter). The presented railing system provides an effective continuous flow methodology to achieve bead-based and cell-based microfluidic reactors for applications including point-of-care (POC) molecular diagnostics, pharmacological screening, and quantitative cell biology.

Introduction

A wide range of chemical and biological assays (*e.g.*, immunoassays) require multi-stage fluidic mixing processes.[1–3] Microfluidic platforms are ideally suited for performing multi-stage mixing operations with numerous fluidic reagents and washes due to scaling-induced benefits, such as low reagent volumes, rapid reaction times, and precise control of micro-environmental conditions.[4–6] Particulate-based microfluidic systems offer additional advantages for accomplishing biochemical assays, including high surface-to-volume ratios, low costs, and the ability to mix-and-match microparticles corresponding to specific screenings.[7–11] In particular, microbead substrates can be functionalized with a variety of molecular diagnostic probes in order to detect target biomolecules, such as DNA analytes and inflammatory cytokines.[12–14] At present, biochemical assays primarily utilize fluidic mixing routines in which multiple reagents and/or washes are loaded independently in set orders.[15] Methods for executing such processes can be exceedingly limited (*e.g.*, in terms of time and labor), which has led to the recent development of microfluidic systems with automated ''on-chip'' functionalities, including device-embedded flow switching, clocking functions, and logic operations.[16–18]

Microfluidic railing systems that are capable of transporting suspended microbeads and cells into discrete, parallel flow streams (*i.e.*, under continuous input flow conditions) could be utilized to autonomously accomplish multi-stage particulate-based reaction processes. Previously, microfluidic railing systems have been demonstrated for photopatterned microstructures and microdroplets.[19–21] For example, researchers have used opto-fluidic lithography techniques to rail (*i.e.*, guide) a variety of photopolymerized microstructures within microfluidic systems by using a second layer that acts as a 'track.'[21–25] Multi-layer photolithographic processes have also been used to etch grooves into microchannels in order to rail microdroplets (*i.e.*, by taking advantage of the physical properties associated with droplet surface energy).[19] To bypass the limitations associated with multi-layer fabrication processes (*e.g.*, increased costs, time and labor), researchers have also developed single-layer microfluidic systems for railing microdroplets using comparatively smaller microposts (alternatively referred to as micropillars).[20] In the area of molecular diagnostics, researchers have found that the distance between surface-immobilized detection probes and corresponding substrates (*e.g.*, microbeads) can be adjusted *via*

[a]*Department of Mechanical Engineering, University of California, Berkeley, USA. E-mail: rsochol@gmail.com; Fax: +1 510 643 6637; Tel: +1 410 935 8971*
[b]*Department of Bioengineering, University of California, Berkeley, USA*
[c]*Berkeley Sensor and Actuator Center (BSAC) and Biomolecular Nanotechnology Center (BNC), University of California, Berkeley, USA*

† Electronic Supplementary Information (ESI) available: Conceptual illustrations and results for device microfabrication, COMSOL Multiphysics models and fluid dynamics simulations, experimental results for limiting diffusion-based mixing and immobilizing select numbers of microbeads within devices, and movies of microbead and cell handling. See DOI: 10.1039/c2lc40610a

This journal is © The Royal Society of Chemistry 2012

extended biological linkers in order to improve probe performance;[26–30] however, current methods for synthesizing biological linkers, such as those consisting of biotin-avidin pairs, suffer from tedious procedures associated with mixing particles with multiple fluidic reagents and washes.[30,31] Because such mixing and washing routines are ubiquitous throughout chemical and biological applications, methodologies that reduce the operational time and labor required to perform multi-stage fluidic processes are in critical demand.

In this work, we present a micropost array railing (μPAR) system for passively guiding suspended microbeads and cells into distinct, adjacent flow streams using continuous input flow sources (Fig. 1). Specifically, microposts arrayed at an angle, "α," with respect to the flow direction, serve as a railing system for directing suspended microparticles into different fluidic streams of reagents and washes. Both theoretical and experimental approaches were employed to investigate the effects of α on railing performance. For continuous input flow conditions, a multiplexed μPAR system was designed to: (*i*) distribute a single inputted microbead suspension into four separate bead-sets, (*ii*) synthesize four distinct extended biological linkers (*i.e.*, consisting of one, two, three, or four biotin-avidin pairs) onto suspended streptavidin-coated polystyrene microbead substrates in parallel, (*iii*) simultaneously bind a fluorescently-labelled analyte onto each bead-set, and (*iv*) ultimately immobilize the suspended microbeads in designated array positions for fluorescence visualization and quantification. The experimental results were analysed in order to elucidate the effects of each extended biological linker length on the fluorescence response of the bead-immobilized fluorescently-labelled analytes. Additionally, experiments with suspended bovine aortic endothelial cells (BAECs) were performed to investigate the efficacy of employing the μPAR system for potential cellular applications.

Materials and methods

Micropost array railing (μPAR)

The μPAR technique consists of square-shaped microposts (*i.e.*, of approximately the same size as the target microparticles) that are arrayed at an angle, "α," with respect to the direction of the inputted fluid flow (Fig. 1a). When a microparticle suspension is loaded into a μPAR system with a sufficiently low value of α, the arrayed microposts serve as a 'track' for physically railing the microparticles into the discrete, parallel fluidic streams (*i.e.*, without altering the primary direction of the inputted fluid flow) (Fig. 1b). For higher values of α, the potential for microparticles to immobilize in the gaps between microposts increases, which can lead to microparticle clogging and device failure (Fig. 1c). By tuning α, microparticle immobilization in the microfluidic system can be passively regulated (*i.e.*, to prevent or promote microparticle immobilization in the spaces between microposts). Furthermore, additional reagents and/or washes can be loaded in parallel as desired to facilitate fluidic mixing of suspended microparticles with higher numbers of adjacent solutions under continuous input flow conditions.

Parallel microbead functionalization *via* μPAR

Previously, researchers have reported that the length between molecular detection probes and microbead substrates can significantly affect probe performance.[26–29] Here, a multiplexed μPAR system was designed to investigate the effects of extended biological linker length on the detectable intensity of bead-immobilized fluorescent analytes. Under continuous flow conditions, six input solutions/suspensions were loaded in parallel, including a suspension of streptavidin-coated microbeads, solutions of biotinylated bovine serum albumin (BSA),

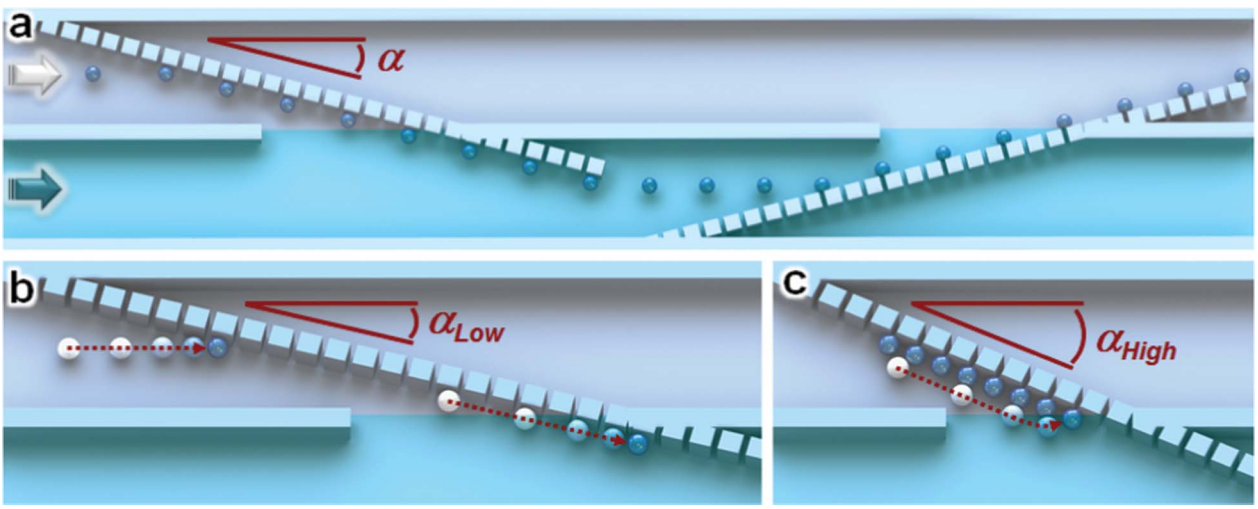

Fig. 1 Conceptual illustrations of the micropost array railing (μPAR) methodology for passively executing multi-stage fluidic mixing reactions with suspended microparticles (*e.g.*, microbeads and cells) under continuous input flow conditions. (a) Square-shaped microposts of approximately the same size as the target microparticles are arrayed at an angle, "α," with respect to the flow direction. The microposts serve as a railing system for guiding suspended particles into discrete, adjacent laminar flow streams of fluidic reagents and/or washes without altering the primary flow directions. Additional flow streams can be loaded in parallel as desired. (b, c) The railing efficiency of the μPAR system can be regulated by tuning α. (b) For μPAR systems with sufficiently low values of α, suspended microparticles are directed into parallel fluidic streams without being immobilized in the gaps between microposts. (c) By increasing α, higher proportions of suspended microparticles can be immobilized in the gaps between arrayed microposts. Illustrations are not to scale.

NeutrAvidin, and biotinylated fluorescent aptamers (FAs), and two wash solutions of phosphate buffered saline (PBS).

The PBS wash solutions limit undesired mixing of the fluidic reagents. By adding or removing μPAR sets (*i.e.*, to increase or decrease the number of times microbeads are mixed with the fluidic reagents and washes), higher or lower numbers of biotin-avidin pairs can be functionalized onto the streptavidin-coated microbead substrates, respectively. For example, Fig. 2a–d show conceptual illustrations of a μPAR methodology for simultaneously conjugating extended biological linkers consisting of one and two biotin-avidin pairs onto streptavidin-coated microbeads in parallel. Initially, the single inputted microbead suspension is hydrodynamically separated into two distinct bead-sets (Fig. 2b). The micropost array rails facilitate the sequential transport of the bottom bead-set into adjacent fluidic solutions of biotinylated BSA and NeutrAvidin (*i.e.*, separated by a wash solution) in order to functionalize the streptavidin-coated microbead substrates with one biotin-avidin pair (Fig. 2c). Thereafter, the same methodology is employed to functionalize a second biotin-avidin pair onto the bottom bead-set while a single biotin-avidin pair in functionalized onto the top bead-set (*i.e.*, by using two sets of micropost array rails in parallel) (Fig. 2d). Both bead-sets are then directed into the biotinylated FA solution. Differing biological linker lengths can result in varying fluorescent intensities for surface-immobilized fluorescent analytes. Conceptual illustrations of the multi-stage reaction process for synthesizing an extended biological linker consisting of four biotin-avidin pairs onto the surface of streptavidin-coated microbead substrates are shown in Fig. 2e. The railing process facilitates the repeated, sequential mixing of the suspended streptavidin-coated microbeads with parallel solutions of biotinylated BSA and NeutrAvidin in order to increase the length of the extended biological linker one 'layer' at a time *via* biotin-avidin binding interactions. The multiplexed μPAR system was designed to simultaneously functionalize streptavidin-coated microbeads with one, two, three, or four biotin-avidin pairs in parallel. At the end of the biological linker synthesis process and subsequent mixing with the solution of biotinylated FAs, each set of microbeads were immobilized in separate array positions (*i.e.*, for fluorescence visualization and signal detection) *via* a previously reported hydrodynamic micropost array trapping (μPAT) technique.[31] At maximum, the reaction process for synthesizing an extended biological linker consisting of four biotin-avidin pairs and a FA onto a streptavidin-coated microbead substrate involves 18 discrete fluidic stages (*i.e.*, including eight wash steps) (Fig. 2e). Experiments in which one, two, three, and four biotin-avidin pairs (and FAs) were conjugated to separate sets of streptavidin-coated microbeads in parallel comprised a total of 48 discrete fluidic stages (*i.e.*, including 20 wash steps).

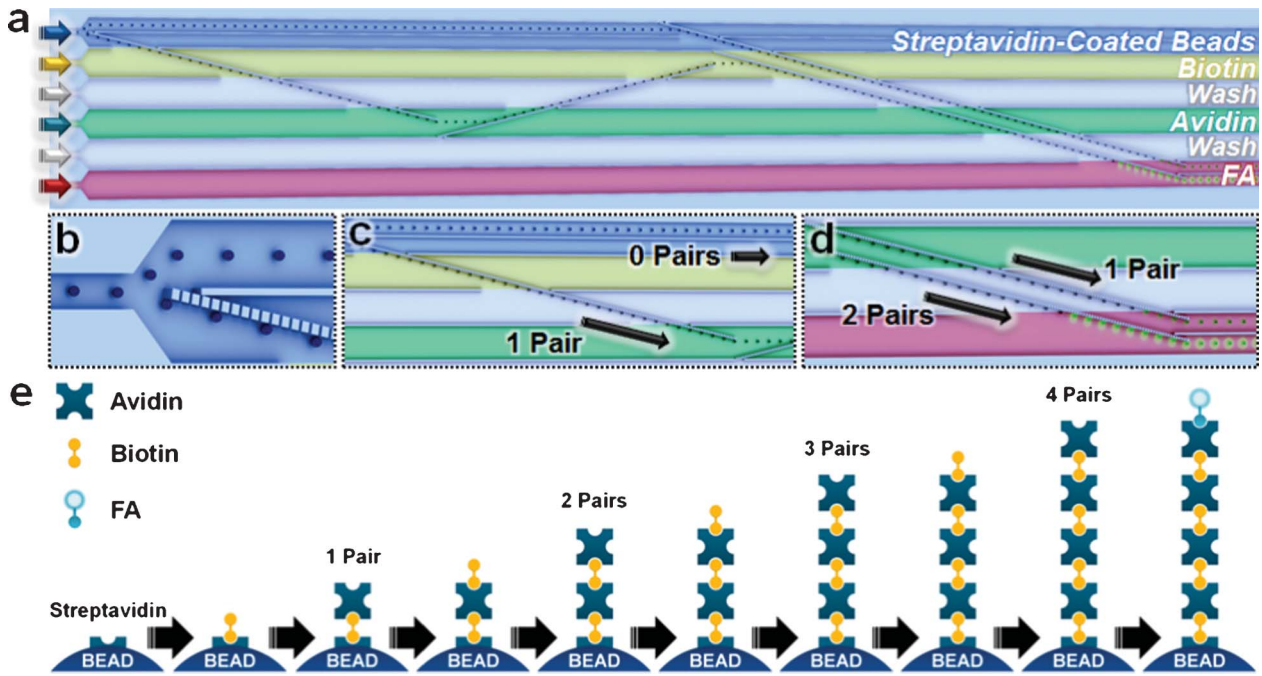

Fig. 2 Conceptual illustrations of a μPAR system for simultaneously synthesizing multiple biotin-avidin pairs, as well as a biotinylated fluorescent aptamer (FA), onto distinct sets of streptavidin-coated microbead substrates in parallel. (a) Distinct, homogenous fluidic suspensions, reagents, and washes are simultaneously loaded into the μPAR system under continuous input flow conditions. The microbeads are passively transported into discrete flow streams in order to functionalize the microbeads with either one or two biotin-avidin pairs, as well as a biotinylated FA. (b–d) Expanded views of the μPAR reaction process. (b) A single inputted microbead suspension is hydrodynamically separated into two distinct bead-sets. (c) Initially, only the *bottom* bead-set is functionalized with one biotin-avidin pair. (d) Thereafter, a second biotin-avidin pair is functionalized onto the *bottom* bead-set while a single biotin-avidin pair in functionalized onto the *top* bead-set. Differing biological linker lengths can result in varying fluorescent intensities for surface-immobilized fluorescent analytes. (e) The multi-stage reaction process (*i.e.*, not including wash steps) for synthesizing an extended biological linker consisting of four biotin-avidin pairs and a biotinylated FA onto a streptavidin-coated microbead substrate. Branching effects associated with biotin-avidin binding interactions are not illustrated. All illustrations are not to scale.

This journal is © The Royal Society of Chemistry 2012

Microfabrication

The microdevices were fabricated *via* a standard soft lithography process as shown in ESI Fig. 1.† The negative photoresist, SU-8 2010 (MicroChem, Newton, MA), was spin-coated onto clean 4″ Silicon wafers. Microfeatures were defined *via* contact photolithography (Hybralign, Series 400, Optical Associates, Milpitas, CA). Using the developed photoresist as a negative master, the devices were micromolded with the silicone elastomer, poly(-dimethylsiloxane) (PDMS), at a 10 : 1 (base : curing agent) ratio (Sylgard 184, Dow Corning, Corning, NY). After curing at 55 °C for at least two hours, the PDMS was removed from the wafer and individual devices were cut from the PDMS. SEM micrographs of fabrication results are shown in ESI Fig. 2a, b.† Ports for all of the catheter couplers (Instech Laboratories, Plymouth Meeting, PA) were punched at inlet and outlet locations. The PDMS devices were cleaned and covalently bonded to glass microscope slides (Fisher Scientific, Pittsburgh, PA) *via* UV ozone treatment (UVO cleaner, model 42, Jetlight Company, Irvine, CA).

The devices were designed for 15.2 μm diameter streptavidin-coated polystyrene microbeads (#SVP-150-4, Spherotech, Inc., Lake Forest, IL) and suspended BAECs (approximately 13–17 μm in diameter on average). Due to the polydispersity of the microbeads and cells, the heights of the microchannels were set at 18 μm. A filter was integrated into the inlet to limit exceptionally large/deformed microparticles and debris from entering the microchannels. The microposts were 15 $\times$ 15 μm^2, and the gaps between microposts were 5 μm (*see* ESI Fig. 2a, b†). Two different μPAR systems were fabricated, including: (*i*) a testing system for experimentally investigating varying values of α (*i.e.*, 30°, 20°, 10°, 5°, 2.5°, and 1°) on μPAR efficiency, and (*ii*) a multiplexed system for synthesizing four distinct extended biological linkers onto microbead substrates in parallel (α = 1°). A photograph of the multiplexed μPAR system filled with coloured dye solutions is shown in ESI Fig. 2c.†

Fluid velocity field simulations

Three-dimensional fluid velocity field simulations were modelled using the commercial finite element analysis software, COMSOL Multiphysics Version 3.5a (COMSOL, Inc., Burlington, MA). The three-dimensional 'Incompressible Navier–Stokes' application mode for steady-state analysis was used for all of the simulations. Each μPAR model (corresponding to varying α) included a sphere (15 μm in diameter) placed in contact with the corners of two arrayed microposts in the center of the width of a channel. An experimentally relevant input fluid velocity was set at 2.3 mm s^{-1} for all of the velocity field simulations. The pressure at the outlet of each system was set at 0 Pa, while all other boundary conditions were set to have no-slip conditions. Water (ρ = 103 kg m^{-3}; $\mu = 10^{-3}$ Pa•s) was modelled in all of the fluid dynamics simulations. All simulations included mesh sizes of at least 4 $\times$ 10^4 elements. A sample mesh is shown in ESI Fig. 3.†

Experimental reagents and suspensions

Both the biotinylated BSA and NeutrAvidin reagents (Sigma-Aldrich Corporation, St. Louis, MO) were used in order to maintain consistency with prior work.[31] For the PBS washes, GIBCO™ Dulbecco's 1X PBS (#14287072, Invitrogen Corp., Carlsbad, CA) was used. The biotinylated FAs, which form the basis of a previously reported diagnostics probe,[12] were terminally labelled with fluorescein (FAM) on the 5′ end of the aptamer (6-FAM-TGGGGTTGGTTGTGTTGGGTGTT-GTGT). The biotinylated FAs were purchased from Biosearch Technologies, Inc. (Novato, CA). All of the experimental reagents were used without further purification or amplification.

For experiments with suspended microbeads, 15.2 μm diameter streptavidin-coated polystyrene microbeads (Spherotech) were used. For experiments with cells, suspensions of BAECs were prepared *via* standard cell culture techniques.[32] For visualization purposes, the actin proteins of the BAECs used in this study were transfected with mCherry fluorescent proteins (#632522, Clontech Laboratories, Inc., Mountain View, CA). Both the microbead and cell suspensions were loaded at concentrations of approximately 100 microparticles/μL, which were the highest concentrations found to enable particle loading without inducing microparticle clogging at the inlet locations (*i.e.*, prior to entering the μPAR systems), such as from too many microparticles entering the microchannels simultaneously.

Experimental setup

All microbead-based experiments were conducted under room temperature environment (20–25 °C) and without thermal cycling during device operation. Prior to device operation, the polysorbate surfactant, Tween 20 (10% in PBS, Fisher), was vacuum loaded into all of the devices for a 15 min incubation period. For the μPAR α testing experiments, three syringe pumps were used to control the input flow rates (each set at 0.5 μL min^{-1}) for each homogenous solution or suspension in parallel. For the multiplexed μPAR system, six syringe pumps were used to control the input flow rates (set at 0.6 μL min^{-1} for the PBS wash solutions; 0.5 μL min^{-1} for all other input solutions/suspensions) during parallel, continuous flow loading of the homogenous fluids. Experimental testing was concluded after approximately 30 min, corresponding to reagent/suspension volumes of 15 μl and PBS wash solution volumes of 18 μl. To determine the fluorescence response of streptavidin-coated microbeads without biological linkers after mixing with the FA solution (*i.e.*, for the negative control), the biotin and avidin solutions were replaced with PBS washes. The negative control experiments were also run using the multiplexed μPAR device. For cell handling experiments with the μPAR system, BAECs (suspended at 37 °C in CO_2 independent media, Invitrogen) were loaded into the "α = 1°" testing system in parallel with a blue-dyed PBS wash solution and a red-dyed PBS wash solution *via* separate inlet ports. Three syringe pumps were used to control the input flow rates (set at 0.5 μL min^{-1}) for each dyed PBS wash solution and the cell media suspension.

Diffusion considerations

For the multiplexed μPAR system, several design and experimental considerations were utilized in order to limit the potential diffusion of reagents through the wash solutions (*i.e.*, resulting in undesired solution-phase mixing). The μPAR systems were designed with walls (10 μm in width) separating parallel solutions

in order to prevent mixing; however, openings (approximately 3 mm in length) were necessary to enable microparticle transport between adjacent solutions. Potential solution-phase mixing would require diffusion from both the biotinylated BSA and NeutrAvidin solutions – each over a distance equivalent to half the width of the PBS microchannel (and the wall opening). Because the microchannels and wall openings were set at 200 μm and 10 μm, respectively, the diffusion distance was 105 μm. Assuming diffusion coefficients of approximately 60 $\mu m^2\ s^{-1}$ for both the biotinylated BSA and the NeutrAvidin reagents,[33,34] the diffusion time over a distance of 105 μm is 92 s.[31] To limit reagent consumption in the device without sacrificing particle mixing times, the minimum effective input flow rate for the syringe pumps – 0.5 $\mu L\ min^{-1}$ – was used. The low flow rate also served to reduce the corresponding lengths of the microchannels associated with particle mixing, thereby decreasing the overall device footprint. For input flow rates of 0.5 $\mu L\ min^{-1}$, microchannel widths of 200 μm, and microchannel heights of 18 μm, the average fluid velocity within the device is equivalent to 2.3 $mm\ s^{-1}$.[31] Thus, the critical channel length for undesired solution-phase mixing to occur is 21 cm.[31] To account for this distance over the course of the 14 stages of biotin-PBS-avidin interactions within the device (*i.e.*, from the first point of contact between the biotinylated BSA and PBS wash solutions to the final point of contact between the PBS wash and NeutrAvidin solutions), while also maximizing the corresponding particle mixing times, the lengths of the microchannels for each mixing stage were set at approximately 15 mm. Additionally, to further limit undesired solution-phase mixing of the biotinylated BSA and NeutrAvidin solutions, the input flow rates for the PBS wash solutions were set at 0.6 $\mu L\ min^{-1}$. The comparatively higher flow rates of the PBS wash solutions served to displace the mixing interactions of the parallel fluids in order to promote diffusive activity within the biotinylated BSA and the NeutrAvidin microchannels (*i.e.*, instead of within the PBS wash channels) (*see* ESI Fig. 4†).

Data acquisition and analysis

All images were captured using a fluorescent inverted microscope (Motic AE31, Motic, Inc., Richmond, BC, Canada) connected to a Micropublisher 5.0 RTV charge-coupled device (CCD) camera (QImaging Corp., Surrey, BC, Canada) and calibrated with QCapturePro (QImaging). Singular microbeads in motion appear as *orange* and *blue* corresponding to two time-points within one second. After the microbeads or cells were immobilized in the final trapping arrays, fluorescent images were captured at 100X magnification. The freely available software, ImageJ (National Institutes of Health (NIH), Bethesda, MD), was used to quantify the fluorescence response of each arrayed microbead directly from the captured images.

Railing Failure Rates (*RFR*s) associated with the μPAR α testing experiments were quantified as:

$$RFR = \frac{N_B}{N_G} \quad (1)$$

where N_B is the number of microbeads that ultimately immobilized in the gaps between microposts (or on top of previously immobilized microbeads), and N_G is the total number of potential gaps between microposts where the inputted microbeads could have been immobilized. Thus, an ideal microfluidic railing system would yield a *RFR* of 0%, a system in which a single microbead immobilized in every potential gap between microposts would yield a *RFR* of 100%, and a system in which microbeads consistently immobilized on top of other previously immobilized microbeads would yield a *RFR* greater than 100%. The *RFR* experimental results were quantified from approximately 250 microbeads loaded into each α testing system (*i.e.*, for an approximate total of 1,500 microbeads).

To quantify the fluorescence results, the relative fluorescent intensity (*RFI*) for each individual microbead was calculated as:

$$RFI_i = x_i - \overline{x_S} \quad (2)$$

where x_i is the fluorescent intensity of a single microbead, and $\overline{x_S}$ is the mean fluorescent intensity of the microbeads without any biotin-avidin pairs (*i.e.*, with only streptavidin) for the corresponding experiment. The calculation of *RFI* values normalized the fluorescence results such that the mean *RFI* for the streptavidin (*negative control*) case was normalized to 0. The fluorescence results were quantified from approximately 350 arrayed microbeads from five distinct bead-based experimental device runs. Because microbead-microbead contact can distort the fluorescence response,[31] data were excluded for microbeads that were in contact with other arrayed beads (or not immobilized in the designated trapping positions). Quantified experimental results are presented in the text as mean $\pm$ s.e.m. The p values corresponding to differences in *RFI* were calculated *via* unpaired *Student's t tests* because the fluorescence results associated with each biotin-avidin pair were not assumed to be distinct. Differences with p values that were less than 0.05 were considered statistically significant.

Results

Effects of α on railing performance

Three-dimensional COMSOL Multiphysics fluid dynamics simulations were performed for μPAR systems with values of α varying from 1° to 30° (see ESI Fig. 5†). The simulation results revealed that systems with significantly lower values of α (*i.e.*, $2.5^\circ \geqslant \alpha$) appeared to promote fluid flow along the micropost array rails compared to systems with higher values of α (*i.e.*, $\alpha \geqslant 20^\circ$). These results suggest that decreasing α would reduce the potential for microparticles to remain immobilized in the gaps between microposts, thereby enhancing the corresponding railing efficiency for such systems. Experimental device runs with suspended streptavidin-coated polystyrene microbeads (15 μm in diameter) were performed using μPAR systems with α varying from 1° to 30°. Despite the added resistance associated with the microposts in the channels, the micropost array rails were not found to disrupt the initial flow directions of the inputted fluids. Experimental observations revealed that for higher values of α (*i.e.*, $\alpha \geqslant 20^\circ$), microbeads were not only found to immobilize in the gaps between microposts, but also to array on top of previously immobilized microbeads (Fig. 3a, b). Despite this phenomenon of microbeads forming 'layers' to varying degrees, full microbead clogging was not observed during experimental testing. Rather, subsequent beads entering such systems were

 This journal is © The Royal Society of Chemistry 2012

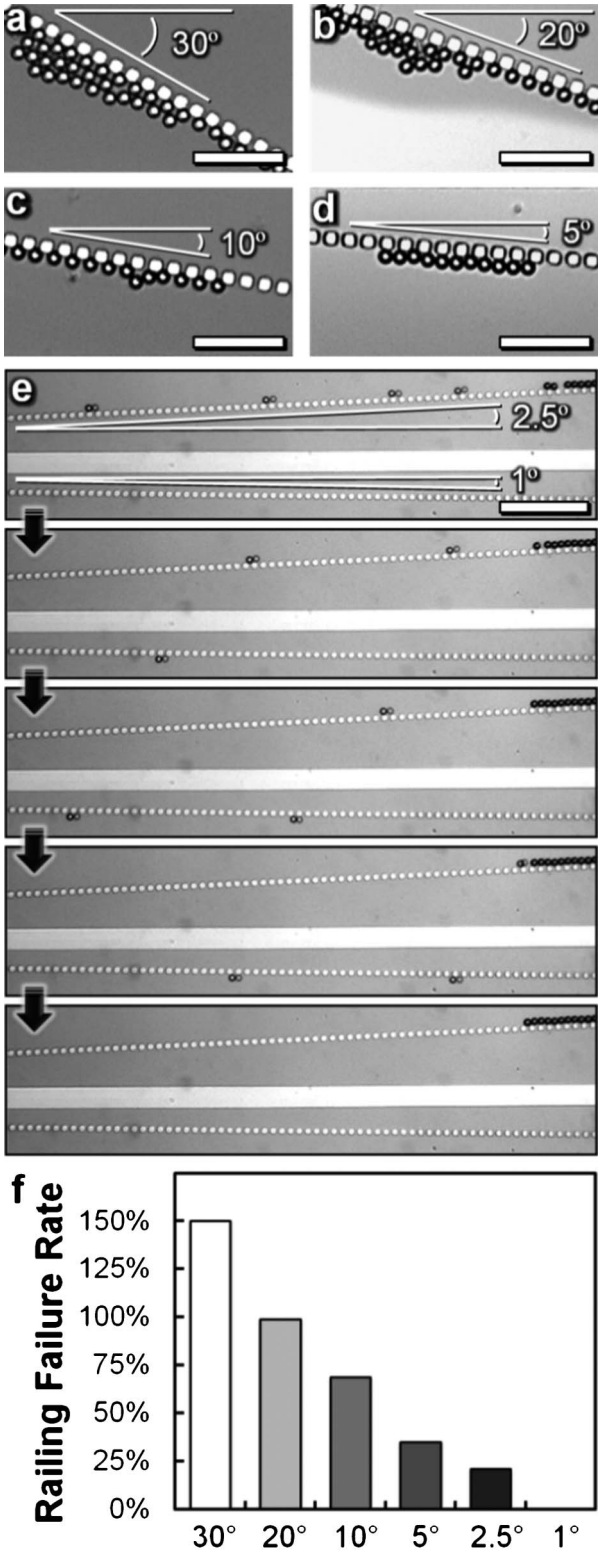

Fig. 3 Experimental results for μPAR systems with varying values of α. (a–d) Micrographs of microbeads immobilized in μPAR systems with: (a) $\alpha = 30^\circ$, (b) $\alpha = 20^\circ$, (c) $\alpha = 10^\circ$, and (d) $\alpha = 5^\circ$. Scale Bars = 100 μm. (e) Sequential micrographs of microbeads railing and then immobilizing in a system with $\alpha = 2.5^\circ$ (*top*), while microbeads are simultaneously railed without being immobilized in a system with $\alpha = 1^\circ$ (*bottom*). Scale Bar = 200 μm. (f) Quantified results for the railing failure rate (*RFR*) corresponding to each value of α tested (n = approximately 250 microbeads for each case). The *RFR*s were calculated *via* eqn (1).

found to eventually bypass the layered microbeads, which prevented microbead clogging in the device. The lack of full microbead clogging was likely due to the added fluidic resistance associated with additional microbead layers obstructing fluid flow through the gaps between microposts. For slightly lower values of α (*i.e.*, $\alpha = 10^\circ$ and $\alpha = 5^\circ$), microbeads were still found to immobilize within the μPAR testing systems (Fig. 3c, d). In addition, microbead immobilization was observed in systems with values of α as low as 2.5°; however, decreasing α further to 1° was found to prevent microbead immobilization completely. For example, Fig. 3e shows sequential micrographs of microbeads being railed and then immobilized in a system with $\alpha = 2.5^\circ$ (*top*), while microbeads are successfully railed in a system with $\alpha = 1^\circ$ (*bottom*). The *RFR*s corresponding to each value of α tested were quantified using eqn (1), and the results are presented in Fig. 3f. The microbead-based experimental device runs revealed that the failure rate decreased as α was reduced. The system with $\alpha = 1^\circ$ was the only μPAR system tested in which microbead immobilization was not observed (*i.e.*, *RFR* = 0%). Rather, suspended microbeads were guided along the micropost array rails into the discrete, parallel flow streams. Although full microbead clogging was not observed for any of the values of α tested, the loss of microbeads in μPAR systems can be detrimental to device performance. Railing failure directly limits the microbead processing throughput, thereby increasing the time, volume of reagents, and number of beads associated with each experimental run. Microbead immobilization in the gaps between microposts also obstructs the flow of fluid through the gaps, which increases the fluidic resistance within the μPAR system. In addition to necessitating higher input pressures, this resistance was found to dynamically distort the flow patterns of the fluids during the particle loading process (Fig. 3b). During experimental testing, $\alpha = 1^\circ$ was the only value of α found to preclude all of these limitations.

Autonomous synthesis of four distinct extended biological linkers onto microbead substrates in parallel

For the synthesis of four extended biological linkers (*i.e.*, consisting of one, two, three, or four biotin-avidin pairs) in parallel, a multiplexed μPAR system with an α of 1° was used. Experimental device runs revealed that after dividing the inputted microbead suspension into four separate bead-sets, the micropost array rails successfully directed the microbeads through the distinct reagents and wash solutions as designed. For example, Fig. 4a–d show sequential micrographs of experimental results for microbeads being passively transported from: (a) the microbead suspension (*blue*) to the biotinylated BSA solution (*yellow*), (b) the biotinylated BSA solution (*yellow*) to the PBS wash solution (*white*), (c) the PBS wash solution (*white*) to the NeutrAvidin solution (*green*), and (d) the NeutrAvidin solution (*green*) back to the PBS wash solution (*white*). ESI Movie 1† shows real-time video of this process. In the multiplexed μPAR system, streptavidin coated-microbeads were mixed with the biotinylated BSA and NeutrAvidin solutions as designed to simultaneously functionalize the microbead substrates with one, two, three, or four biotin-avidin pairs in parallel. After fluidic mixing with the FA solution, each set of microbeads were immobilized in separate trapping arrays for fluorescence visualization and signal detection. Experimental

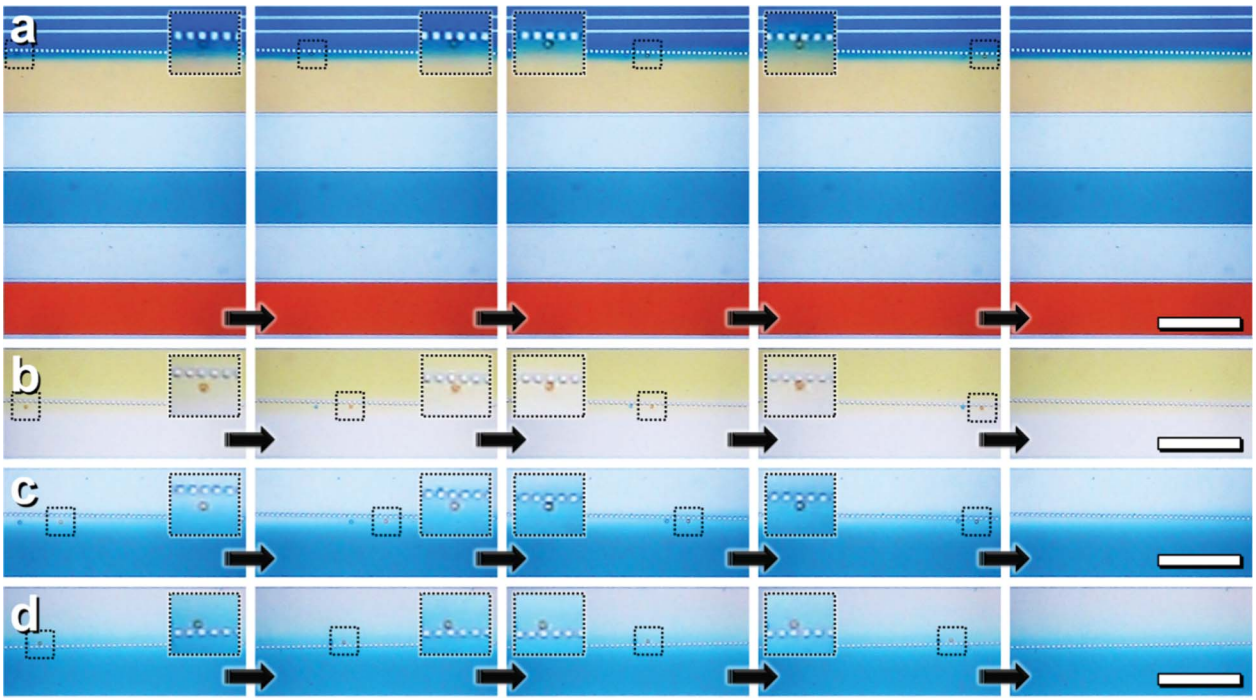

Fig. 4 Sequential micrographs of experimental results for microbead dynamics in the multiplexed μPAR system. Suspended streptavidin-coated polystyrene microbeads (15 μm in diameter) are transported from: (a) the microbead suspension (*blue*) to the biotinylated bovine serum albumin (BSA) solution (*yellow*), (b) the biotinylated BSA solution (*yellow*) to the phosphate buffered saline (PBS) wash solution (*white*), (c) the PBS wash solution (*white*) to the NeutrAvidin solution (*green*), and (d) the NeutrAvidin solution (*green*) back to the PBS wash solution (*white*). *Insets* show enlarged views of suspended microbeads; *Orange* and *blue* microbeads show a singular mobile microbead captured at two time-points within one second; Dyed suspension/solution colours are for visualization purposes only; Scale Bars = 300 μm. ESI Movie 1 shows real-time video of this process.†

observations revealed that the micropost array rails decreased the microbead velocities to approximately 10% of the average velocity of the fluid flow, resulting in each bead-based fluidic mixing stage occurring for approximately one minute. Consequently, the full reaction process was accomplished over a time-span of roughly 18 min. This marks a significant improvement in terms of time and labor compared to off-chip processes of prior works, such as those that require over 45 min (and 50 μl of each reagent) to conjugate biological linkers with only a single biotin-avidin pair to streptavidin-coated microbead substrates.[31] During experimental runs, a microbead processing rate of approximately 50 beads min^{-1} was observed.

Fig. 5a–e show fluorescence micrographs of arrayed 15 μm diameter streptavidin-coated microbeads corresponding to: (a) zero biotin-avidin pairs (*i.e.*, for the negative control), (b) one biotin-avidin pair, (c) two biotin-avidin pairs, (d) three biotin-avidin pairs, and (e) four biotin-avidin pairs. Solution-phase FAs were found to produce background noise in all of the cases (Fig. 5a–e); however, fluorescence quantification was not prevented (Fig. 5f). Microbead *RFI* values were quantified using eqn (2) and the fluorescence results are shown in Fig. 5f. The experimental results revealed that as the length of the extended biological linker increased up to three biotin-avidin pairs, the corresponding *RFI* increased as well. After mixing with the FA solution, microbeads with one biotin-avidin pair produced an average *RFI* of 48.3 $\pm$ 10.3, which was significantly higher than the negative control microbeads ($p < 0.0001$). The addition of a second biotin-avidin pair resulted in a further increase in microbead fluorescence ($p < 0.05$), with an average *RFI* of 91.4 $\pm$ 15.2. The highest fluorescence intensities were observed for microbeads with three biotin-avidin pairs. Specifically, the average *RFI* for streptavidin-coated microbeads with three biotin-avidin pairs was 138.0 $\pm$ 10.4, which was significantly higher than the two-pair case ($p < 0.05$) and the one-pair case ($p < 0.0001$). Conversely, the addition of a fourth biotin-avidin pair resulted in a significant decrease in microbead fluorescence ($p < 0.0001$). After mixing with the FA solution, streptavidin-coated microbeads with four biotin-avidin pairs produced an average *RFI* of 41.5 $\pm$ 10.1. Although this response was significantly higher compared to the control case ($p < 0.0005$), the fluorescence intensities for the four-pair case were not statistically discernible from the one-pair case ($p = 0.64$) (Fig. 5f). This observed trend is consistent with prior works that have found that increasing the lengths of extended biological linkers beyond an optimal distance can result in a decrease in the fluorescence response.[27] These results suggest that further research is needed to elucidate the potential molecular mechanisms (*e.g.*, branching interactions associated with biotin-avidin binding, bead-based quenching, *etc.*) that could account for the observed relationship between biological linker length and fluorescence performance.

Autonomous mixing of suspended cells with discrete, parallel flow streams

The capability of employing the μPAR technique to transport suspended cells into distinct, adjacent flow streams under continuous flow conditions was experimentally investigated.

This journal is © The Royal Society of Chemistry 2012

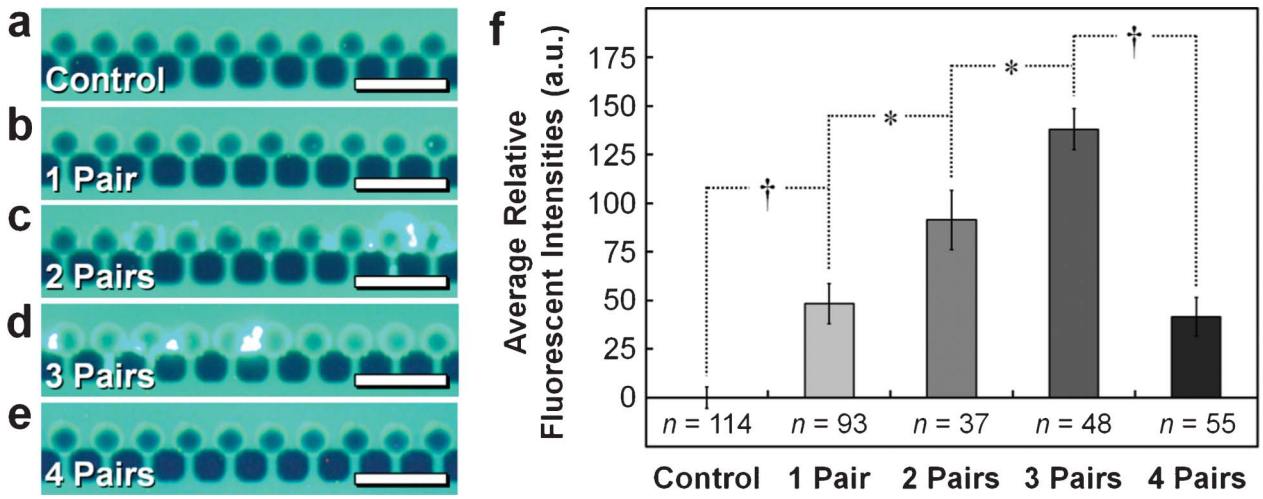

Fig. 5 Experimental results for microbead fluorescence *versus* biological linker length. (a-e) Fluorescence micrographs of streptavidin-coated polystyrene microbeads (15 μm in diameter) immobilized *via* a micropost array trapping (μPAT) technique[31] corresponding to: (a) zero biotin-avidin pairs (*i.e.*, the negative control), (b) one biotin-avidin pair, (c) two biotin-avidin pairs, (d) three biotin-avidin pairs, and (e) four biotin-avidin pairs. Scale Bars = 50 μm. (f) Average relative fluorescent intensities (*RFIs*) of arrayed microbeads after mixing with the FA solution. The *RFI* values were quantified *via* eqn (2). Error Bars denote s.e.m.; * and † denote $p < 0.05$ and $p < 0.0001$ statistically significant differences, respectively.

Suspended BAECs were loaded into a μPAR testing system with $\alpha = 1^{\circ}$. Experimental testing revealed that the μPAR system effectively transported suspended cells into the parallel flow streams of blue-dyed and red-dyed PBS wash solutions, with an observed *RFR* equivalent to 0% (n = approximately 250 cells). For example, Fig. 6a–c show sequential micrographs of suspended BAECs being railed between the cell media suspension, a blue-dyed PBS wash solution, and a red-dyed PBS wash solution (*see* ESI Movie 2† for real-time video of this process). After transporting the suspended BAECs back into the red-dyed PBS wash solution, the cells were immobilized in the designated array positions for brightfield and fluorescence visualization (Fig. 6d, e). These results demonstrate that the μPAR methodology could be integrated into cell-based microfluidic

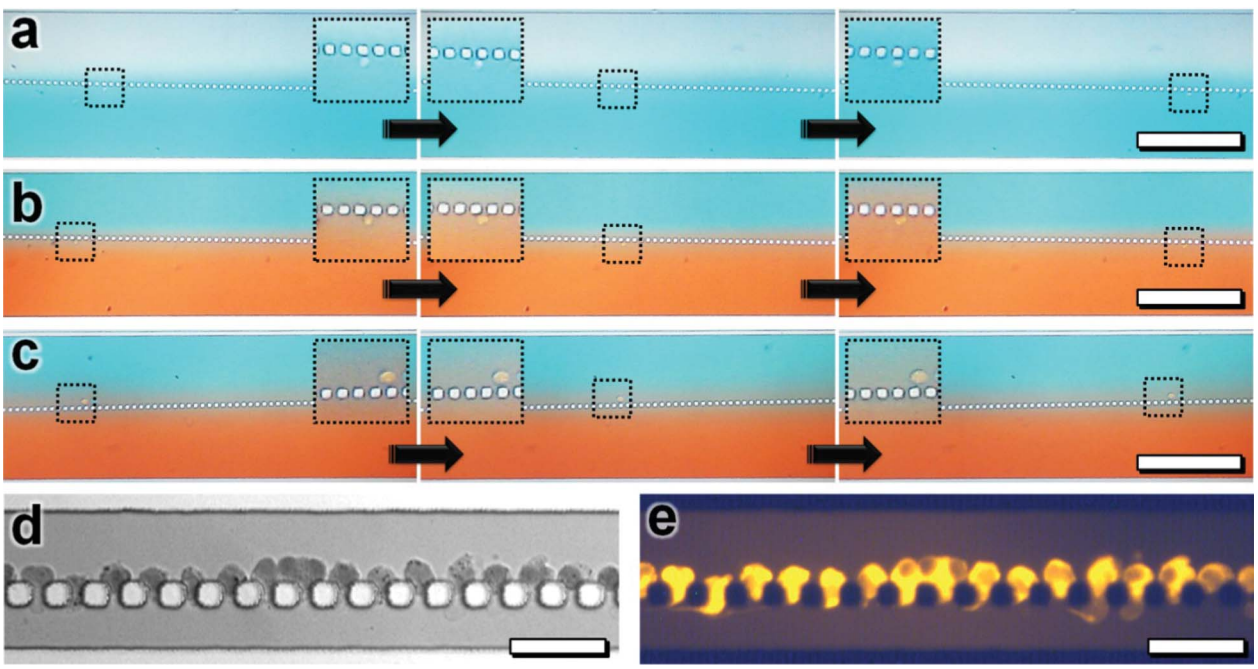

Fig. 6 Experimental results for cell handling in a μPAR system. (a–c) Sequential micrographs of bovine aortic endothelial cells (BAECs) being transported from: (a) the cell media suspension (*white*) to a blue-dyed PBS wash solution, (b) a blue-dyed PBS wash solution to a red-dyed PBS wash solution, and (c) a red-dyed PBS wash solution back to the blue-dyed PBS wash solution. Insets show enlarged views of suspended cells; Dyed suspension/solution colours are for visualization purposes only; Scale Bars = 300 μm. ESI Movie 2† shows real-time video of this process. (d, e) Identical micrographs of BAECs immobilized in μPAT array positions after being directed back into the red-dyed PBS wash solution under (e) brightfield and (f) fluorescence microscopy. Scale Bars = 50 μm.

processors to autonomously mix suspended cells with discrete solutions of fluidic reagents and washes under continuous input flow conditions.

Conclusions

The ability to autonomously perform multi-stage fluidic mixing operations on-chip directly impacts the advancement of microfluidic platforms for chemistry and biology, such as POC biochemical detection, biomarker discovery, and cellular diagnostics. Here, a single-layer microfluidic μPAR system was developed to passively transport suspended microbeads and cells into discrete, parallel flow streams of fluidic reagents and washes using continuous input flow sources. Both theoretical and experimental approaches revealed that decreasing the angle α limited the immobilization of suspended microparticles within the μPAR system, thereby improving the corresponding railing efficiency. In particular, microposts arrayed at an angle of 1° from the flow direction were found to effectively transport suspended microbeads and cells into discrete, adjacent flow streams under continuous input flow conditions.

In this work, the μPAR technique was employed to simultaneously synthesize four distinct extended biological linkers (*i.e.*, consisting of one, two, three, or four biotin-avidin pairs) onto streptavidin-coated polystyrene microbead substrates in parallel. In addition, the four bead-sets were mixed with a fluorescently-labelled analyte, resulting in detectable fluorescent intensities on the surface of the microbeads. To accomplish these fluidic assays for the four separate bead-sets, a total of 48 discrete fluidic mixing stages were passively executed in parallel on-chip. At maximum, the reaction process for synthesizing an extended biological linker consisting of four biotin-avidin pairs as well as a FA onto a streptavidin-coated microbead substrate included 18 sequential fluidic mixing stages. During experimental device runs, the micropost array rails were observed to guide the suspended microbeads into the multiple, adjacent fluidic reagents and washes as designed. Quantified experimental results revealed that the fluorescence response was enhanced as the length of the extended biological linker increased up to three biotin-avidin pairs; however, the addition of a fourth biotin-avidin pair was found to decrease the fluorescence response. These results are in agreement with prior studies that have reported that the length of biological linkers can be tuned in order to maximize the fluorescent intensities of substrate-immobilized detection probes.[26–29] Although the fluidic mixing processes in this work (*i.e.*, consisting of up to 18 fluidic stages) were performed over a time-span of 18 min, input flow rates and channel geometries can be adjusted in order to increase or decrease particulate-based fluidic mixing times as desired. Additionally, the presented μPAR system was designed to examine the fluorescence performance of select numbers of microbeads for a given experiment, rather than to enhance the overall microbead processing throughput. For potential applications that demand high-throughput functionalization of microbeads, a variety of experimental conditions (*e.g.*, input flow rates, microparticle concentrations, and device geometries) can be modified to maximize microparticle processing rates accordingly.

Here, suspended microbeads and cells were immobilized exclusively after all of the microfluidic mixing reactions; however, the μPAR technique can be adapted for applications that necessitate microparticle visualization and fluorescence detection at intermediate steps over the course of multi-stage reaction processes. For example, by varying the angle at which the microposts are arrayed with respect to the direction of the fluid flow (*e.g.*, from 1° to 15°), a select number of microparticles can be immobilized within the μPAR system during specified reaction-stages (*see* ESI Fig. 6†). Additionally, the microfluidic systems in this work were designed with microparticles and microposts that were approximately the same size, which suggests that the presented technique could be scaled up or down as desired (*i.e.*, to handle particles of various sizes).

Acknowledgements

The authors greatly appreciate the contributions of Ryan Ruelos, Valerie Chang, William Krieger, Kosuke Iwai, Adrienne Higa, Julia Chu, Liana Lo, Joanne Lo, Paul Lum, the Liwei Lin Laboratory, the Biologically-inspired Photonics-Optofluidic-Electronic Technology and Science (BioPOETS) group, and the Micro Mechanical Methods for Biology (M^3B) Laboratory Program. This work is supported in part by the DARPA N/MEMS program under the Micro/Nano Fluidics Fundamentals Focus (MF3) center.

References

1 C. D. Chin, T. Laksanasopin, Y. K. Cheung, D. Steinmiller, V. Linder, H. Parsa, J. Wang, H. Moore, R. Rouse, G. Umviligihozo, E. Karita, L. Mwambarangwe, S. L. Braunstein, J. van de Wijgert, R. Sahabo, J. E. Justman, W. El-Sadr and S. K. Sia, *Nature Medicine*, 2011, **17**, 1015-U1138.
2 D. A. Giljohann and C. A. Mirkin, *Nature*, 2009, **462**, 461–464.
3 T. Tachi, N. Kaji, M. Tokeshi and Y. Baba, *Lab Chip*, 2009, **9**, 966–971.
4 P. Yager, T. Edwards, E. Fu, K. Helton, K. Nelson, M. R. Tam and B. H. Weigl, *Nature*, 2006, **442**, 412–418.
5 T. Thorsen, S. J. Maerkl and S. R. Quake, *Science*, 2002, **298**, 580–584.
6 A. D. Tadmor, E. A. Ottesen, J. R. Leadbetter and R. Phillips, *Science*, 2011, **333**, 58–62.
7 K. Iwai, W.-H. Tan, H. Ishihara and S. Takeuchi, *Biomed. Microdevices*, 2011.
8 W. H. Tan and S. Takeuchi, *Proc. Natl. Acad. Sci. U. S. A.*, 2007, **104**, 1146–1151.
9 W. H. Tan and S. Takeuchi, *Lab Chip*, 2008, **8**, 259–266.
10 J. H. Wang, W. Wang, Y. H. Liu, L. B. Duo, L. J. Huang and X. F. Jiang, *Mol. Biol. Rep.*, 2008, **36**, 1903–1908.
11 E. Verpoorte, *Lab Chip*, 2003, **3**, 60N–68N.
12 N. Tuleuova, C. N. Jones, J. Yan, E. Ramanculov, Y. Yokobayashi and A. Revzin, *Anal. Chem.*, 2010, **82**, 1851–1857.
13 S. A. Dunbar, *Clin. Chim. Acta*, 2006, **363**, 71–82.
14 F. J. Steemers and K. L. Gunderson, *Biotechnol. J.*, 2007, **2**, 41–49.
15 D. C. Appleyard, S. C. Chapin, R. L. Srinivas and P. S. Doyle, *Nat. Protoc.*, 2011, **6**, 1761–1774.
16 D. C. Leslie, C. J. Easley, E. Seker, J. M. Karlinsey, M. Utz, M. R. Begley and J. P. Landers, *Nat. Phys.*, 2009, **5**, 231–235.
17 B. Mosadegh, C.-H. Kuo, Y.-C. Tung, Y.-s. Torisawa, T. Bersano-Begey, H. Tavana and S. Takayama, *Nat. Phys.*, 2010, **6**, 433–437.
18 J. A. Weaver, J. Melin, D. Stark, S. R. Quake and M. A. Horowitz, *Nat. Phys.*, 2010, **6**, 218–223.
19 P. Abbyad, R. Dangla, A. Alexandrou and C. N. Baroud, *Lab Chip*, 2011, **11**, 813–821.
20 C. Kantak, S. Beyer, L. Yobas, T. Bansal and D. Trau, *Lab Chip*, 2011, **11**, 1030–1035.
21 S. E. Chung, W. Park, S. Shin, S. A. Lee and S. Kwon, *Nat. Mater.*, 2008, **7**, 581–587.
22 S. E. Chung, Y. Jung and S. Kwon, *Small*, 2011, **7**, 796–803.
23 S. E. Chung, S. A. Lee, J. Kim and S. Kwon, *Lab Chip*, 2009, **9**, 2845–2850.

 This journal is © The Royal Society of Chemistry 2012

24 S. H. Lee, S.-E. Choi, A. J. Heinz, W. Park, S. Han, Y. Jung and S. Kwon, *Small*, 2010, **6**, 2668–2672.
25 W. Park, H. Lee, H. Park and S. Kwon, *Lab Chip*, 2009, **9**, 2169–2175.
26 S. Shimozono and A. Miyawaki, *Methods Cell Biol.*, **85**, 381.
27 G. Yao and W. H. Tan, *Anal. Biochem.*, 2004, **331**, 216–223.
28 Z. R. Zhu, J. Chao, H. Yu and A. S. Waggoner, *Nucleic Acids Res.*, 1994, **22**, 3418–3422.
29 B. H. Kwon, B. H. Choi, H. M. Lee, Y. J. Jang, J. C. Lee and S. K. Kim, *Bull. Korean Chem. Soc.*, 2010, **31**, 1615–1620.
30 D. Horejsh, F. Martini, F. Poccia, G. Ippolito, A. Di Caro and M. R. Capobianchi, *Nucleic Acids Res.*, 2005, 33.
31 R. D. Sochol, B. P. Casavant, M. E. Dueck, L. P. Lee and L. Lin, *J. Micromech. Microeng.*, 2011, **21**, 054019.
32 R. D. Sochol, A. T. Higa, R. R. R. Janairo, S. Li and L. Lin, *Soft Matter*, 2011, **7**, 4606–4609.
33 N. Muramatsu and A. P. Minton, *Proc. Natl. Acad. Sci. U. S. A.*, 1988, **85**, 2984–2988.
34 J. R. Wayment and J. M. Harris, *Anal. Chem.*, 2009, **81**, 336–342.